AJNR Am J Neuroradiol 21:928–931, May 2000

Technical Note

A High-resolution Fast Spin-echo Inversion-recovery Sequence for Preoperative Localization of the Internal Globus Pallidus

Caroline A. Reich, Patricia A. Hudgins, Scott K. Sheppard, Philip A. Starr, and Roy A.E. Bakay

Summary: A fast spin-echo inversion-recovery (FSE-IR) sequence is described for its utility regarding surgical planning for patients with Parkinson's disease (PD) who are undergoing microelectrode-guided internal globus pallidus (GPi) ablation. Images from thirty-seven adult patients with PD were reviewed and visualization of the GPi, globus pallidus externa (GPe), and the intervening lamina was noted. High-resolution images were acquired from all patients despite the external hardware and the patients' movement disorder. In all cases, the conventional surgical trajectory, determined indirectly by a fixed measurement from the anteroposterior commissure line, was modified by the ability to visualize the GPi and optic tract directly. This sequence facilitated accurate stereotactic targeting.

Surgical ablation of the internal globus pallidus (GPi) has become an accepted treatment for patients with medically intractable Parkinson's disease (PD) (1–3), a disorder characterized by rigidity, akinesia, tremor, and postural instability (4). MR imaging that can accurately reveal the GPi within the basal ganglia is used to aid in preoperative planning (5). The imaging allows direct visualization of the GPi, which should optimize anatomic planning because the stereotactic coordinates can be obtained by directly measuring from the boundary of the GPi, bypassing the problems associated with a variable GPi location. The purpose of this study was to evaluate a fast spin-echo inversion-recovery (FSE-IR) sequence used for preoperative planning among patients undergoing GPi ablation for PD. The ability of this sequence to resolve the boundaries of the GPi and the potential artifacts of the sequence were determined. The FSE-IR sequence was also compared with the previously used gradient-echo or fast field–echo (FFE) sequence (5) to assess differences in contrast, contrast-to-noise ratios (CNRs), and relative contrast-to-noise ratios (RCNR) in the region of the globus pallidus (GP).

Received August 4, 1999; accepted after revision December 10.

From the Greystone Imaging Center, University of Birmingham, Alabama; the Departments of Radiology (P.A.H.) and Neurosurgery (R.A.E.B.), Emory University School of Medicine, Atlanta; Philips Medical Systems (S.K.S.); and the Department of Neurosurgery (P.A.S.), University of California, San Francisco.

This paper was presented at the American Society of Neuroradiology, Toronto, Canada, May 1997.

Address reprint requests to P.A.Hudgins, MD, Division of Neuroradiology, Department of Radiology, Emory University School of Medicine, 1364 Clifton Road, NE, Atlanta, GA 30322.

Description of Technique

Subjects Analyzed

Over a 7-month period, 37 consecutive adult patients were carefully assessed clinically and determined by the neurologists and neurosurgeons to be candidates for the pallidotomy procedure. Inclusion criteria required the diagnosis of idiopathic PD with two of the following cardinal signs: rigidity, bradykinesia, tremor, or postural instability and a prior history of a good response to levodopa. In addition, an unsatisfactory clinical response to maximal medical management must have developed. Contraindications to pallidotomy included significant dementia, extensive brain atrophy, ''Parkinson's-plus'' syndromes (such as postencephalitic or posttraumatic parkinsonism) or preexisting disorders that would increase the risk of postoperative complications (eg, coagulopathies, uncontrolled hypertension). An initial MR study was performed as a part of the screening protocol to detect signs of secondary PD, significant atrophy, or hydrocephalus. The candidates included 20 men and 17 women, ranging in age from 20 to 79 years, with a mean age of 60 years.

Frame Placement

For MR-guided target localization, the Leksell Series G stereotactic system (Eleckta, Atlanta, GA) was used. The frame is aluminum and is attached to the head with titanium pins. For preoperative images and the intraoperative instrument trajectories to occur in standard anatomic planes, precise and reproducible frame placement was required. Determination of target coordinates required that the images obtained be parallel to one of the axes of the frame as well as parallel or orthogonal to the anterior commissure–posterior commissure (AC-PC) line. Using the Leksell stereotactic frame in the absence of surgical-planning software, it is necessary to align images orthogonally to the frame axes. To achieve these goals, the neurosurgeon adjusted the anteroposterior or *y* axis of the frame so that it was parallel to a line drawn from the inferior orbit to the external auditory meatus, which in turn was approximately parallel to the AC-PC line (6). The frame and localizer were then fitted with a cylindrical adapter, allowing the frame to fit snugly into the head coil.

Pulse Sequence Evaluation

All antiparkinsonian medications were withheld after midnight prior to surgery, and each patient was scanned using the FSE-IR preoperative sequence on the day of surgery.

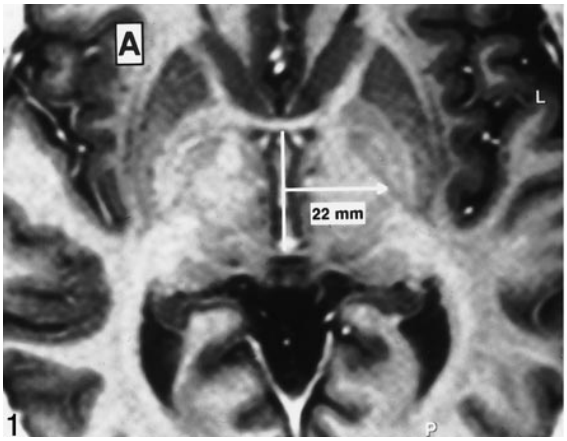

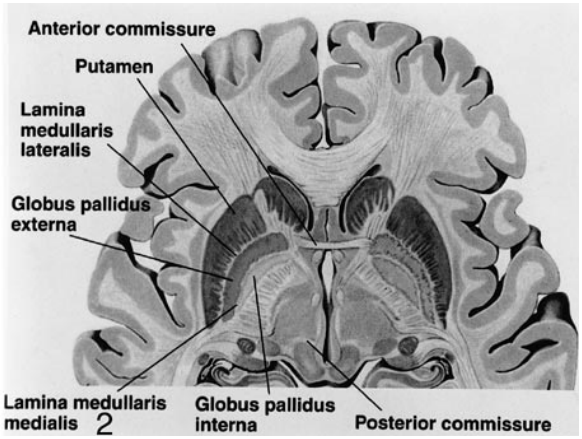

FIG 1. Axial FSE-IR image [3000/40/4 (TR/TE/excitations), with TI 200 ms, echo train length 5, 2 mm slice thickness] through the basal ganglia. Conventional localization of the GPi is a point 22 mm lateral to the midportion of the AC-PC line. This approach does not take into account the normal variations in laterality of the GPi.

FIG 2. Anatomy of the GP. Axial diagrammatic depiction of the GPi from the GPe. The ''lamina medullaris medialis'' is synonymous with the GPi-GPe lamina (Borrowed with permission from Cohn and colleagues. Pre- and postoperative MR evaluation of stereotactic pallidotomy. AJNR 1998;19:1075–1080.).

MR images were acquired on a 1.5-T magnet, using a FSE-IR sequence with the following parameters: 3000/40/2 or 4 (TR/TE/excitations), TI = 200 ms, echo train length = 5, 2-mm slice thickness, and no interslice gap. Four excitations were used for axial images (time of acquisition, 19 min), and two excitations were used for coronal images (time of acquisition, 8.5 min). A 256 × 230 matrix was used with interpolated reconstructions of 512 × 512. Axial and coronal images were displayed using real-image reconstruction.

Two radiologists retrospectively reviewed the images obtained using this sequence, noting visibility of the GPi, globus pallidus externa (GPe), GPi-GPe lamina, and optic tract and evaluating the presence of artifacts.

Ten healthy adult volunteers with no history of neurologic disease were imaged using the FSE-IR protocol described above (using two excitations) and an FFE sequence that was previously used in the preoperative pallidotomy protocol (33/4.5/2, flip angle = 35, 1.5-mm slice thickness, and no interslice gap). Operator-defined region-of-interest (ROI) measurements of signal intensity were obtained from the GP, caudate nucleus, and frontal lobe white matter bilaterally in all volunteers by using both imaging sequences. Four standardized, representative ROIs were placed in each area, and the values were averaged. The value for background noise was obtained by placing a large rectangular ROI over the entire image background ventral to the patient.

Detection of the GP required sufficient contrast or signal intensity difference between the nucleus and surrounding tissue. The following formulas were used to calculate contrast between the GP and the caudate nucleus (C_{CN}) and between the GP and white matter (C_{WM}):

$$C_{CN} = S_{GP} - S_{CN}/S_{GP}; \quad (7)$$
$$C_{WM} = S_{GP} - S_{WM}/S_{GP}$$

Furthermore, the ability to resolve small differences in the GP and surrounding tissues was limited by random variations in image signal intensity that was reflected in the standard deviation of background noise. Therefore, CNRs were also calculated as follows:

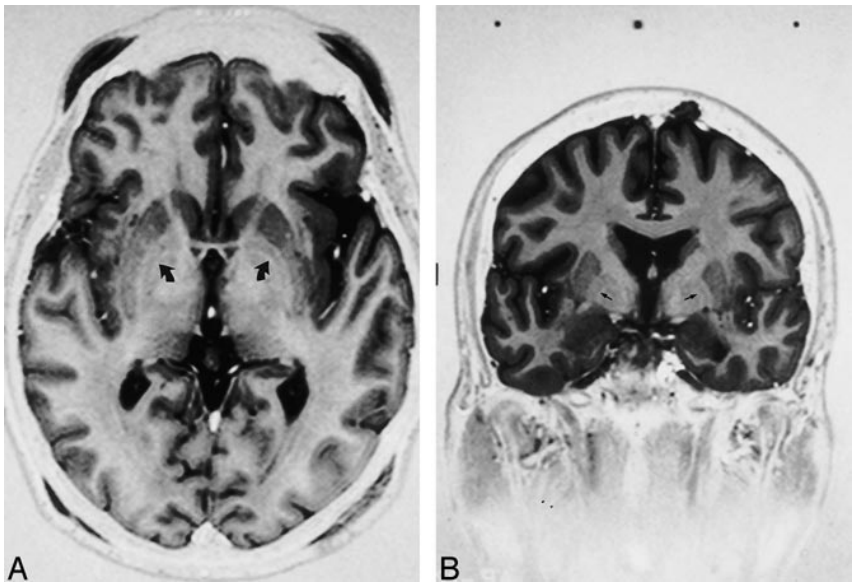

FIG 3. Axial (*A)* and coronal (*B*) fast spin-echo inversion-recovery sequences [3000/40/2–4, TI = 200 ms, echo train length = 5, 2-mm slice thickness] show GPi-GPe lamina (*small arrows*), separating the GPi from the GPe. On the axial image, the posterior commissure is not seen. The frame placement technique described only approximates the AC-PC line.

TABLE 1: Contrast assessment

	Contrast		Contrast to Noise	
	GP/WM	GP/CN	GP/WM	GP/CN
FSE-IR	0.32 +/− 0.06	0.45 +/− 0.08	8.7 +/− 2.3	11.8 +/− 1.9
FFE	0.14 +/− 0.05	0.15 +/− 0.04	6.2 +/− 1.9	7.2 +/− 2.8

(8) $CNR_{CN} = S_{GP} - S_{CN}$/SD noise;
$CNR_{WM} = S_{GP} - S_{WM}$/SD noise

Because numeric contrast and CNR values for any sequence can vary over a number of studies, sequence performance was also compared on a subject-by-subject basis using relative contrast (RC) and RCNRs. Relative contrast for the white matter (WM) was determined by dividing the value for contrast between the GP and white matter obtained by the FSE-IR sequence by that from the FFE protocol for each subject. The relative contrast between the caudate nucleus (CN) and GP was obtained in a similar manner. RCNRs were calculated in a manner similar to that used to determine relative contrast values, using the individual subjects' CNR from each sequence.

$$RC_{WM} = C_{WM}(\text{FSE-IR})/C_{WM}(\text{FFE})$$
(per subject)
$$RC_{CN} = C_{CN}(\text{FSE-IR})/C_{CN}(\text{FFE})$$
(per subject)
$$RCNR_{WM} = CNR_{WM}(\text{FSE-IR})/CNR_{WM}(\text{FFE})$$
(per subject)
$$RCNR_{CN} = CNR_{CN}(\text{FSE-IR})/CNR_{CN}(\text{FFE})$$
(per subject)

A ratio greater than 1 indicates superior performance of the FSE technique for that lesion (8). High-resolution images were acquired from all patients. Axial images were obtained from all patients, and coronal images were acquired in 35. The fiducial markers of the headframe were identified on the films, but no artifact was present that degraded the images. Although all patients had a movement disorder, no significant motion artifact was seen on any images.

Results

The GP is composed of two segments divided by a thin line, the GPe-GPi lamina. Standard atlases have been used to determine the distance of the GPi from the midline (Fig 1) but have not taken into account the individual variation in this measurement. The GPi is medial to the lamina and the GPe is lateral (Fig 2). In 35 of 37 axial images acquired nearest the plane of the AC-PC line, the GPe-GPi lamina was visualized (Fig 3A). In 31 of 35 coronal images obtained near the midpoint of the AC-PC line, the lamina and optic tract could be visualized (Fig 3B).

The contrast values and CNRs comparing the GP to the frontal lobe white matter and GP to the caudate nucleus were greater when the FSE-IR sequence was compared with the FFE protocol. (Table 1). The mean and standard deviations for the RC and RCNR were then calculated and are shown in Table 2. By both qualitative and quantitative measures, FSE-IR allowed enhanced visualization of the boundaries of the posterolateral GPi compared with that obtained by the previously used FFE protocol.

Discussion

Precise placement of the pallidotomy lesion in the posterolateral GPi is of critical importance to achieve optimal alleviation of symptoms (1, 2). The target for ablation, the sensorimotor region, is immediately adjacent to the optic tract and internal capsule. Preoperative imaging, which allows direct visualization of the target nucleus, should aid in surgical planning to enhance lesion accuracy and reduce surgical complications.

To optimize lesion placement, a combination of microelectrode mapping and stereotactic anatomic targeting is used to determine the precise aim. The number of microelectrode tracks required for target determination depends on the accuracy of the initial stereotactic anatomic information. Stereotactic coordinates are used to determine the trajectory of the first microelectrode pass. If the first trajectory is optimized, then fewer subsequent passes should be needed to obtain a complete electrophysiologic map. Microelectrode mapping is used to identify and delineate the caudal sensorimotor portion of the GPi as well as to locate critical nearby structures, such as the optic tract and internal capsule. Although mapping adds to the precision of the procedure, it is invasive and greatly increases operating time. One microelectrode pass can take from 15 to 45 minutes.

TABLE 2: Relative contrast and CNR

	Relative Contrast		RCNR	
	GP/WM	GP/CN	WM	CN
FSE-IR/FFE	2.7 +/− 0.8	3.3 +/− 1.0	1.5 +/− 0.4	1.9 +/− 0.6

Note.—The superior performance of the FSE-IR protocol is demonstrated by the values for relative contrast ratios and RCNRs that are >1.

The advantage of the FSE-IR MR protocol is that it provides direct visualization of the boundaries of the GPi so that the accuracy of stereotactic localization is increased. Previously, MR imaging was used as an indirect guide for GPi localization. Relatively fixed measurements from the midpoint of the AC-PC line were used to estimate the location of the GPi (1–3). Direct visualization of the boundaries of the GPi allows more precise determination of the stereotactic coordinates. Using the high-resolution sequence, the *x* and *y* coordinates are determined on the axial scan at the level of the AC-PC line by measuring the area approximately 4 mm medial from the GPi-GPe lamina. The *z* coordinate is obtained from the coronal image nearest the midpoint of the AC-PC line at the superior border of the optic tract.

The geometric distortion that can result from magnetic field inhomogeneities related to the presence of a headframe represents a potential limitation to the use of MR imaging for the determination of stereotactic coordinates. The headframe used in this series of patients has been shown to cause minimal image distortion (9).

Unlike conventional spin-echo imaging, inversion-recovery sequences can generate two types of images—a ''real'' and a ''modulus'' image. Modulus images are typically used in conventional spin-echo and gradient-echo imaging and are produced from the square root of the sum of the squares of the detected magnetization (10). Therefore, if there were any negative longitudinal magnetization present, this would not be apparent in the typical T1 modulus image. Real-image reconstruction allows the negative component of the magnetization to be represented. Our images were displayed using ''real-image reconstruction,'' which is preferred by the neurosurgeon. One disadvantage of the real-image reconstruction is that the fiducial markers may vary in signal intensity, and surgical planning software (if used) may not recognize all the markers (6).

In conclusion, FSE-IR MR imaging has improved resolution of the basal ganglia so that the boundaries of the GPi can be directly visualized, even in a patient with a movement disorder imaged in a headframe. Preoperative images to guide surgical localization can be acquired within a reasonable time on the day of surgery. Contrast, CNRs, and relative contrast values indicate the superior performance of FSE-IR for the detection of the GP compared with that of the previously used FFE sequence. The ability to visualize the GP reliably is clinically significant, because it allows modification of the conventional stereotactic approach, thereby optimizing anatomic targeting.

References

1. Baron, MS, Vitek JL, Bakay RA, et al. **Treatment of advanced Parkinson's disease by posterior GPi pallidotomy: 1-year results of a pilot study.** *Ann Neurol* 1996;40:355–366
2. Iacono RP, Shima F, Lonser RR, et al. **The results, indications, and physiology of posteroventral pallidotomy for patients with Parkinson's disease.** *Neurosurgery* 1995;36:1128–1127
3. Laitinen LV, Bergenheim T, Hariz MI. **Leksell's posteroventral pallidotomy in the treatment of Parkinson's disease.** *J Neurosurg* 1992;76:53–61
4. Adams RD, Victor M. ***Principles of Neurology*.** 5th ed. New York, NY: McGraw-Hill, Inc;1993;975–982
5. Cohn MC, Hudgins PA, Sheppard SK, Starr PA, Bakay RAE. **Pre- and postoperative MR evaluation of stereotactic pallidotomy.** *AJNR Am J Neuroradiol* 1998;19:1075–1080
6. Starr PA, Vitek JL, DeLong M, Bakay RAE. **Magnetic resonance imaging-based stereotactic localization of the globus pallidus and subthalamic nucleus.** *Neurosurgery* 1999;44:303–313
7. Taupitz M, Speidel A, Hamm B, Deimling M, Reichel M, Bock A, Wolf K-J. **T2-weighted breath-hold MR imaging of the liver at 1.5T: results with a three-dimensional steady-state free precession sequence in 87 patients.** *Radiology* 1995;194:439–446
8. Rydberg JN, Lomas DJ, Coakley KJ, Hough DM, Ehman RL, Riedere SJ. **Comparison of breath-hold fast spin-echo and conventional spin-echo pulse sequences for T2-weighted MR imaging of liver lesions.** *Radiology* 1995;194:431–437
9. Burchiel KJ, Nguyen TT, Coombs BD, Szumoski J. **MRI distortion and stereotactic neurosurgery using the Cosman-Roberts-Wells and Leksell frames.** *Stereotact Funct Neurosurg* 1996;66:123–136
10. Bernstein MA, Thomasson DM, Perman WH. **Improved detectability in low signal-to-noise ratio magnetic resonance images by means of a phase-corrected real reconstruction.** *Med Phys* 1989;:16:813–817